Peculiar Ferrimagnetism Associated with Charge Order in Layered Perovskite $GdBaMn_2O_{5.0}$

A. A. Taskin and Yoichi Ando

Central Research Institute of Electric Power Industry, Komae, Tokyo 201-8511, Japan
(Received 11 February 2007; published 14 May 2007)

The magnetic properties of $GdBaMn_2O_{5.0}$, which exhibits charge ordering, are studied from 2 to 400 K using single crystals. In a small magnetic field applied along the easy axis, the magnetization M shows a temperature-induced reversal which is sometimes found in ferrimagnets. In a large magnetic field, on the other hand, a sharp change in the slope of $M(T)$ coming from an unusual turnabout of the magnetization of the Mn sublattices is observed. Those observations are essentially explained by a molecular field theory which highlights the role of delicate magnetic interactions between Gd^{3+} ions and the antiferromagnetically coupled Mn^{2+}/Mn^{3+} sublattices.

Ferrimagnetism is a complex but intriguing type of magnetic ordering. It occurs when antiferromagnetically aligned spins have different local moments, resulting in their incomplete cancellation. The characteristics of this type of ordering stem from the fact that it combines features of both ferromagnetic (FM) and antiferromagnetic (AF) systems. Moreover, if more than two spin sublattices are involved, a new level of complexity, and hence new physics, can emerge [1]. So far, only a few families of ferrimagnetics with three magnetic sublattices—spinel ferrites, and rare-earth garnets being the most famous examples [2]—have been discovered. These materials are proved to be not only fundamentally interesting, but also technologically important [3], inspiring the search for new promising magnetic compounds.

Recently, half-doped *A*-site ordered manganite perovskites $RBaMn_2O_{5+x}$ (where R is a rare-earth element) have been synthesized in an effort to clarify the role of the random potential effect in the colossal magnetoresistance (CMR) phenomena [4–8]. It has been found that in addition to the interesting electronic properties, these compounds possess another potentially useful quality, a variability of the oxygen content [4–6,9]. By varying the oxygen concentration from $x = 0$ to $x = 1$, one can readily change the valence state of Mn ions from 2+ through 3+ to 4 +, generating a variety of possible magnetic states. In particular, Mn ions adopt two valence states, Mn^{2+} and Mn^{3+}, and develop a charge order in the reduced composition $RBaMn_2O_{5.0}$ ($x = 0$) [4,5]. Since most rare-earth ions (R^{3+}) are also magnetic, $RBaMn_2O_{5.0}$ can be a three-sublattice magnetic system with potentially ferrimagnetic type of ordering; among the rare-earths, Gd with the largest spin and zero orbital angular momentum would make a benchmark compound of this family. It is worth noting that the layered crystal structure of these compounds naturally implies an anisotropy in its magnetic properties and, therefore, single crystals would have a great advantage for studying their magnetic behavior; however, previous studies on $RBaMn_2O_{5.0}$ [4–6] only used polycrystalline samples.

In this Letter, we present the first study of the magnetic properties of $GdBaMn_2O_{5.0}$ single crystals, which show unusual behavior: At $T_N = 144$ K, a long-range order of Mn^{2+} and Mn^{3+} magnetic moments is established. Upon decreasing temperature in a small magnetic field along the c axis, a magnetization reversal occurs at the compensation point T_{comp}, below which the net magnetic moment is opposite to the magnetic-field direction. On the other hand, in a large magnetic field the magnetization M is positive at all temperatures, and shows a sharp kink in the $M(T)$ curve at T_{comp}. We show that the observed magnetic behavior is essentially understood if Gd spins, which remain paramagnetic through T_N and T_{comp}, are weakly coupled ferromagnetically (antiferromagnetically) with Mn^{3+} (Mn^{2+}) neighbors and gradually align their spins parallel (antiparallel) to the Mn^{3+} (Mn^{2+}) sublattice with decreasing T in low fields. What is special here is that in high magnetic fields, due to the weak Gd-Mn coupling, the Gd spins are aligned along the external magnetic field, which eliminates the magnetization reversal; intriguingly, in this situation an abrupt turnabout of the magnetization of the Mn sublattices occurs at T_{comp}, which, to our knowledge, has never been observed in any ferrimagnets. Hence, the peculiar ferrimagnetism in $GdBaMn_2O_{5.0}$ is quite distinct from other transition-metal oxides showing magnetization reversals [1,2,10,11].

The high-quality single crystals of $GdBaMn_2O_{5+x}$ used for this study were grown by the floating-zone technique. The as-grown crystals were annealed in flowing argon-hydrogen mixture at $600\,^{\circ}C$ for several days to obtain the stoichiometry of $x = 0$, which is confirmed by the thermogravimetric analysis. Parallelepiped samples were cut and polished with all faces adjusted to the crystallographic planes to within 1°. Magnetization measurements were carried out using a SQUID magnetometer at fields up to 70 kOe applied parallel or perpendicular to the c axis.

Figure 1 shows the temperature dependences of the magnetization of $GdBaMn_2O_{5.0}$ in a magnetic field of 100 Oe applied parallel or perpendicular to the spin easy
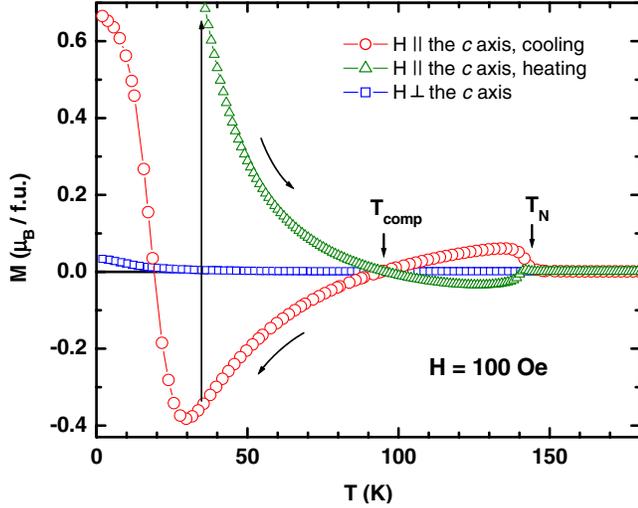
FIG. 1 (color online). Temperature dependences of M under different conditions. Upon cooling in $H = 100$ Oe applied along the c axis (circles), $M(T)$ becomes negative at T_{comp} and eventually returns to positive at lower temperature; upon heating, nearly a "mirror image" is observed after applying a high magnetic field ($H = 3$ kOe at $T = 35$ K for the curve shown by triangles). The squares show $M(T)$ measured in $H = 100$ Oe applied along the ab plane for both cooling and heating.

axis. Upon cooling in a magnetic field along the c axis, $M(T)$ (shown by circles) rapidly increases below the Néel temperature, $T_N = 144$ K, indicating the onset of a magnetic ordering. About 10 K below T_N, $M(T)$ reaches a maximum, then starts to decrease and eventually goes to zero at $T_{\text{comp}} = 95$ K. This temperature, which is called the compensation point, marks the state where magnetic contributions of all sublattices cancel each other. Below T_{comp}, $M(T)$ becomes negative, indicating that the net magnetic moment is opposite to the external magnetic-field direction. This phenomenon is called the temperature-induced magnetization reversal [1,2,10,11].

Upon further decrease in temperature and concomitant development of sublattice magnetizations, the net magnetic moment grows too large to remain in this metastable state. Eventually a magnetic field (even as small as 100 Oe) can overcome the coercive force, leading to a rotation of the net magnetization. As a consequence, another sign change of $M(T)$ occurs at around 20–30 K. The effect of this rotation of the net magnetic moment can be illustrated even more clearly in the following experiment: First, the direction of the sublattice magnetizations in the sample cooled down to an intermediate temperature in 100 Oe are switched by applying a large magnetic field (for example, $H = 3$ kOe at $T = 35$ K as shown in Fig. 1). Then, the magnetic field is reduced down to 100 Oe again and $M(T)$ is measured upon heating. As can be seen in Fig. 1, $M(T)$ shows almost a "mirror image" of the magnetization recorded upon cooling, indicating that the 180°-spin-rotated state is kept intact up to T_N once it is formed.

A comparison of $M(T)$ measured along different crystallographic axes reveals another important feature of the magnetic behavior in GdBaMn$_2$O$_5$: The magnetization is strongly anisotropic with an easy direction along the c axis (see Fig. 1), simplifying significantly a possible arrangement of Mn^{3+}, Mn^{2+}, and Gd^{3+} spins.

In order to obtain further insight into the observed phenomena, the field dependence of the magnetization has been measured at 2 K where the magnetizations of all sublattices are expected to be fully developed. As shown in Fig. 2(a), a magnetic field of about 1 kOe applied along the c axis is enough to reach the saturation. A much higher magnetic field (about 50 kOe) must be applied perpendicular to the easy axis to reach the same saturation level. The equality of the saturation magnetization $M_{\text{sat}} \approx 5.85$ $\mu_B/$f.u. achieved along different crystallographic axes suggests that the obtained value reflects the net saturated moment, which should be simply composed of the sublattice magnetizations.

Obviously, there is a unique combination of spin-only moments of the three spin sublattices—Mn^{3+} ($S_{\text{Mn}^{3+}} = 2$), Mn^{2+} ($S_{\text{Mn}^{2+}} = 5/2$), and Gd^{3+} ($S_{\text{Gd}^{3+}} = 7/2$)—that can be consistent with the experimentally observed value of the saturated magnetization:

$$g\mu_B(S_{\text{Mn}^{3+}} - S_{\text{Mn}^{2+}} + S_{\text{Gd}^{3+}}) = 6\mu_B, \qquad (1)$$

where $g = 2$ is the Landé g factor and μ_B is the Bohr magneton. This equation suggests an AF coupling between Mn^{2+} and Mn^{3+} and a FM (AF) interaction of Gd^{3+} ions with the Mn^{3+} (Mn^{2+}) sublattice. Note that the paramagnetic (PM) contribution of Gd^{3+} alone [shown by the
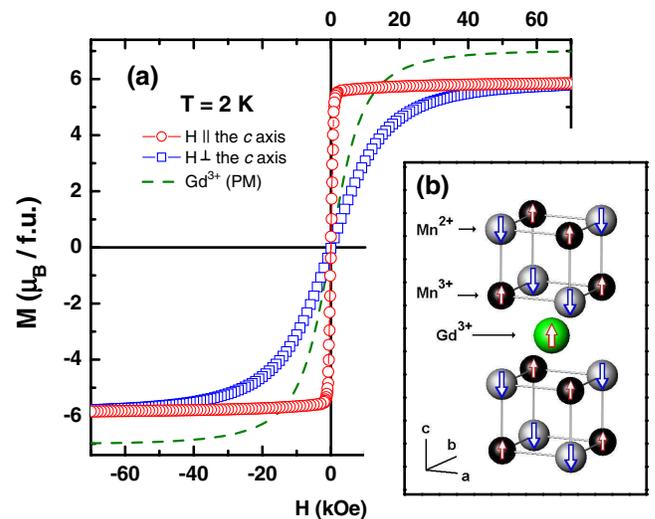

FIG. 2 (color online). (a) $M(H)$ curves of GdBaMn$_2$O$_{5.0}$ with H along the c axis (circles) and the ab plane (squares). The calculated paramagnetic response from the Gd^{3+} sublattice is shown by the dashed line. (b) A sketch of the crystal and magnetic structure of GdBaMn$_2$O$_{5.0}$, showing three magnetic sublattices composed of Mn^{2+}, Mn^{3+}, and Gd^{3+}. Nonmagnetic Ba and O are omitted for the sake of clarity.

dashed line in Fig. 2(a)] would give a larger saturated magnetization than observed. The spin-only magnetic moments of Mn^{3+}, Mn^{2+}, and Gd^{3+} ions are expected to be a good approximation in $GdBaMn_2O_{5.0}$, because the high-spin (HS) Gd^{3+} ($4f^7$) and Mn^{2+} ($3d^5$) have zero orbital angular momentum. For HS-Mn^{3+} ($3d^4$), a state of the e_g symmetry is unoccupied, also implying a lack of the orbital contribution to the total magnetic moment of Mn^{3+}.

Thus, both $M(T)$ and $M(H)$ data point to a ferrimagnetic type of ordering among the three magnetic sublattices of $GdBaMn_2O_{5.0}$. Neutron powder diffraction studies [4,5] as well as density-functional calculations of electronic structure [12,13] have reported a rock-salt arrangement of Mn^{2+} and Mn^{3+} with a G-type AF ordering in $YBaMn_2O_{5.0}$ and $LaBaMn_2O_{5.0}$, compounds with rare-earth ions from opposite ends of the lanthanide series. It would be natural to assume that the same types of charge and magnetic ordering among Mn ions are realized in $GdBaMn_2O_{5.0}$. Magnetic Gd^{3+} ions with a half-filled $4f$ shell are expected to interact ferromagnetically with Mn^{3+} and antiferromagnetically with Mn^{2+} sublattices according to the Goodenough-Kanamori rules [14], although this interaction should be rather weak.

The magnetic structure most likely realized in $GdBaMn_2O_{5.0}$ is shown in Fig. 2(b). Below T_N, Mn^{2+} ($S = 5/2$) and Mn^{3+} ($S = 2$) ions develop a long-range ferrimagnetic order with the spin directions along the c axis. Because of the weak magnetic interaction between Gd^{3+} and Mn^{2+}/Mn^{3+}, the alignment of Gd spins ($S = 7/2$) grows rather slowly with the development of the magnetization of the Mn sublattices below T_N, but eventually almost all Gd spins are aligned along the Mn^{3+} spins at low enough T and add to the large M_{sat}. As can be seen in Fig. 2(a), the magnetization vectors of the ordered sublattices can be 90° rotated by applying a magnetic field of ~50 kOe perpendicular to the easy axis.

Another piece of information about the magnetic behavior of $GdBaMn_2O_{5.0}$ comes from the susceptibility measurements in the paramagnetic phase above T_N. Figure 3 shows the inverse molar susceptibility, measured in $H = 100$ Oe parallel (circles) and perpendicular (squares) to the c axis. Both curves coincide at high temperature, demonstrating the isotropic nature of the paramagnetic phase. In the molecular field theory [1], the temperature dependence of the inverse susceptibility of a three-sublattice ferrimagnetic material above T_N is given by

$$\frac{1}{\chi} = \frac{1}{\chi_0} + \frac{T}{C} - \frac{\sigma(T)}{T - T_N}, \qquad (2)$$

with C the effective Curie constant, T_N the Néel temperature, and $\sigma(T) = (\sigma_0 T + m)/(T + \theta)$; χ_0, σ_0, m, and θ are all constants. The slope of the high-temperature inverse susceptibility shown by the straight dash-dotted line in Fig. 3 is solely given by the effective Curie constant C, which is the sum of the Curie constants of the three magnetic sublattices. The obtained value of 15.1 emuK/mole
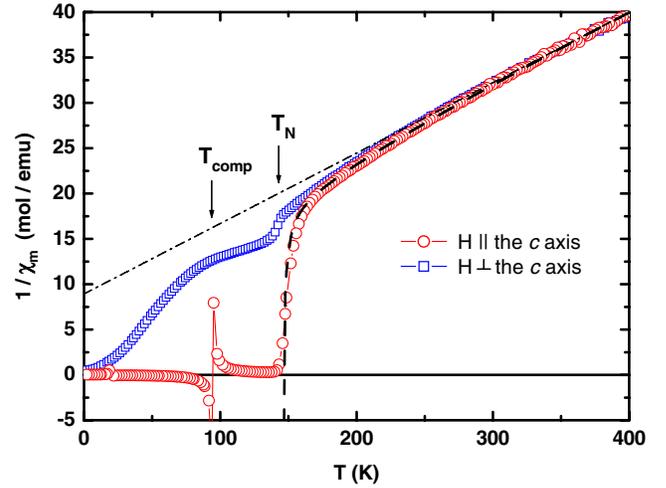

FIG. 3 (color online).   Inverse molar susceptibility $1/\chi_m$, measured in $H = 100$ Oe parallel (circles) and perpendicular (squares) to the c axis, is in agreement with a ferrimagnetic type of ordering. The dashed line is a calculation within the molecular field theory (see text). The dash-dotted line is a guide to the eye.

is only 1% less than what is expected for Mn^{3+} ($S = 2$), Mn^{2+} ($S = 5/2$), and Gd^{3+} ($S = 7/2$) [15], giving further support to the proposed magnetic structure.

When one assumes that only Mn sublattices develop a long-range magnetic order at T_N, the exchange coupling constant J can be estimated, to first approximation, from the following equation [16]:

$$T_N = \frac{q(2 + \alpha + \beta)C_{Mn^{3+}}C_{Mn^{2+}}}{C_{Mn^{3+}} + C_{Mn^{2+}}}, \qquad (3)$$

where $C_{Mn^{3+}}$ and $C_{Mn^{2+}}$ are the Curie constants for Mn^{3+} and Mn^{2+}. Here, $q = (zJ)/(N_a g^2 \mu_B^2)$ is the molecular field constant related to the Mn^{3+}-Mn^{2+} exchange interaction, where $z = 6$ is the number of nearest Mn^{2+} neighbors of Mn^{3+} (and vice versa), N_a is the Avogadro number, and the coefficients α and β give the strengths of the nearest-neighbor exchange interactions in each sublattice of Mn^{3+} and Mn^{2+}, respectively. Note that all constants in Eq. (2) are determined entirely by these exchange interaction parameters and the Curie constants. The fitting curve shown by the dashed line in Fig. 3 is calculated with $J/k_B = 30.5$ K, $\alpha = -0.63$, and $\beta = -0.69$, and it obviously reproduces the data very well, supporting the assumption that Gd spins remain essentially paramagnetic across T_N.

With the obtained exchange interaction parameters, the molecular field theory [1,16] can be applied to the analysis of the temperature dependence of M in the ordered state below T_N. The temperature-induced magnetization reversal observed at low magnetic fields can be reproduced [as shown by the solid line in Fig. 4(a)] only if there is a weak FM (AF) coupling between Gd^{3+} ions and the Mn^{3+} (Mn^{2+}) sublattice. Furthermore, the value of the compensation temperature is very sensitive to the strength of this
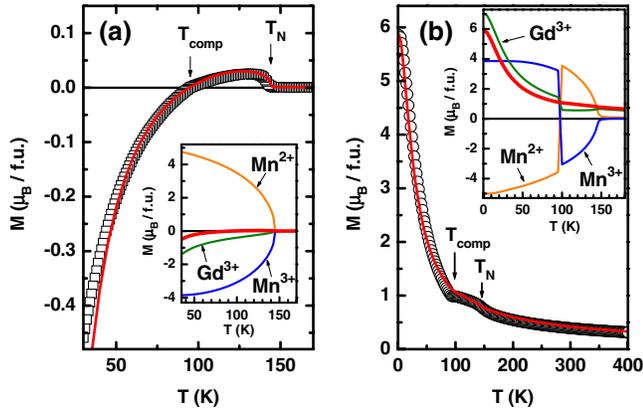
FIG. 4 (color online). Temperature dependence of the easy-axis magnetization in (a) $H = 10$ Oe and (b) $H = 70$ kOe. Solid lines are calculations within the molecular field theory with the same parameters as for Fig. 3 (see text). Insets show the contributions of individual sublattices to the overall magnetization.

interaction. For $T_{comp} = 95$ K, the molecular field constant related to the Gd^{3+}-Mn^{3+} FM exchange is found to be about $0.01q$, i.e., 2 orders of magnitude smaller than the AF exchange interaction between Mn^{3+} and Mn^{2+}. This value corresponds to an effective magnetic field of approximately 35 kOe, while for the ferrimagnetic spin order in the Mn^{3+}/Mn^{2+} sublattices it is ~ 5000 kOe.

The large difference in the exchange interactions between Mn^{3+}-Mn^{2+} and Gd-Mn is crucial for the understanding of the observed magnetic behavior in $GdBaMn_2O_{5.0}$. Just below T_N, Mn^{3+} spins, being antiferromagnetically coupled to the Mn^{2+} sublattice, are opposite to the applied magnetic field, and at low fields Gd spins tend to align in the same direction as the Mn^{3+} sublattice [see inset of Fig. 4(a)], though their alignment is weak; below T_{comp}, the sum of the magnetic moments of Gd^{3+} and Mn^{3+} overgrows the magnetic moment of Mn^{2+}, giving rise to a negative magnetization. Intriguingly, the situation changes completely in a high magnetic field which is strong enough to compete with the Gd-Mn exchange interaction: In this case, Gd spins tend to align along the external magnetic-field direction, causing a positive magnetization at all temperature as shown in Fig. 4(b), and the magnetization reversal is eliminated. It is noteworthy that the Mn spins also behave differently and show a novel turnabout; namely, just below T_N their orientation is the same as in the low magnetic-field case, but with decreasing temperature this state becomes energetically unfavorable as the influence of Gd spins grows. As a result, near the compensation point, an abrupt turnabout of the magnetization of the Mn sublattices takes place [see inset of Fig. 4(b)], which is manifested in the sharp change of the slope of $M(T)$. Note that in the present case the strong Ising anisotropy probably plays a key role in the abrupt turnabout.

To conclude, the present study shows that unusual magnetic behavior of a new three-sublattice ferrimagnetic manganite $GdBaMn_2O_{5.0}$—a temperature-induced magnetization reversal at low magnetic fields and a novel turnabout of Mn sublattice magnetizations at high magnetic fields—are governed by an elaborate interplay between its magnetic sublattices that are formed by the A-site ordering as well as the charge ordering of Mn into Mn^{2+} and Mn^{3+}. In the present case, the weak coupling of Gd spins with magnetically ordered Mn^{2+}/Mn^{3+} sublattices is the source of novel ferrimagnetism not found elsewhere before. This result not only enriches our knowledge about ferrimagnetics, but also points to the potential of charge-order-susceptible transition-metal oxides for discovering physically interesting and technologically useful properties.

[1] L. Néel, Ann. Phys. (Paris) **3**, 137 (1948); Science **174**, 985 (1971).
[2] K. P. Belov, Phys. Usp. **39**, 623 (1996); **42**, 711 (1999); **43**, 407 (2000).
[3] M. Pardavi-Horvath, J. Magn. Magn. Mater. **215–216**, 171 (2000).
[4] F. Millange, E. Suard, V. Caignaert, and B. Raveau, Mater. Res. Bull. **34**, 1 (1999).
[5] F. Millange, V. Caignaert, B. Domengès, B. Raveau, and E. Suard, Chem. Mater. **10**, 1974 (1998).
[6] S. V. Trukhanov, I. O. Troyanchuk, M. Hervieu, H. Szymczak, and K. Bärner, Phys. Rev. B **66**, 184424 (2002).
[7] D. Akahoshi, M. Uchida, Y. Tomioka, T. Arima, Y. Matsui, and Y. Tokura, Phys. Rev. Lett. **90**, 177203 (2003).
[8] Y. Kawasaki, T. Minami, Y. Kishimoto, T. Ohno, K. Zenmyo, H. Kubo, T. Nakajima, and Y. Ueda, Phys. Rev. Lett. **96**, 037202 (2006).
[9] A. A. Taskin, A. N. Lavrov, and Y. Ando, Appl. Phys. Lett. **86**, 091910 (2005).
[10] Y. Ren, T. T. M. Palstra, D. I. Khomskii, E. Pellegrin, A. A. Nugroho, A. A. Menovsky, and G. A. Sawatzky, Nature (London) **396**, 441 (1998).
[11] J. Hemberger, S. Lobina, H.-A. Krug von Nidda, N. Tristan, V. Yu. Ivanov, A. A. Mukhin, A. M. Balbashov, and A. Loidl, Phys. Rev. B **70**, 024414 (2004).
[12] R. Vidya, P. Ravindran, A. Kjekshus, and H. Fjellvåg, Phys. Rev. B **65**, 144422 (2002).
[13] R. Vidya, P. Ravindran, P. Vajeeston, A. Kjekshus, and H. Fjellvåg, Phys. Rev. B **69**, 092405 (2004).
[14] H. Weihe and H. U. Güdel, Inorg. Chem. **36**, 3632 (1997).
[15] The Curie constant C_i of an individual sublattice is $C_i = N_a(g\mu_B)^2 S_i(S_i + 1)/3k_B$, where S_i is the spin of the magnetic ion i.
[16] See, for example, R. Kubo, H. Ichimura, T. Usui, and N. Hashitsume, *Statistical Mechanics: An Advanced Course with Problems and Solutions* (North-Holland, Amsterdam, 1965).